We thank reviewer 2 very much for her/his helpful comments. We took her/his remarks into account and improved the manuscript accordingly.

General comment:

Comment: This study addresses an important teleconnection and an important region that would strongly benefit from better predictions on seasonal timescales. It does however not become clear if this study is able to solve any of the raised issues, and it leaves many open questions as to the methods used and the improvements obtained.

Answer: The East Asian summer monsoon (EASM) is an important and complex climate system. It is composited by different components. How to predict the EASM is a long-standing issue for climate community. This manuscript tries to find the better predictor to predict the EASM and the best initialisation strategy in CMIP5 models for further prediction study. We firstly analysed the seasonal predictability of six variables which contribute to the EASM system. Our finding is that both the lower (850 hPa) and upper (200 hPa) level zonal winds show better prediction skill than monsoon precipitation and meridional winds. A predictor based on the zonal winds might be a good option for EASM prediction. According to previous studies, the Wang and Fan monsoon index outperforms the other monsoon indices in representing the EASM characteristics. Therefore, we chose the Wang and Fan index for further study.

Compared to the non-initialised simulations, the GFDL-CM2p1 and the MIROC5 add prediction skill in simulating the EASM index with initialisation, the BCC-CSM1-1, the CanCM4, and the MPI-ESM-LR change the skill insignificantly, and the HadCM3 indicates a decreased skill score. We tried to answer the different response to the initialisation in the prediction systems. Then, we analysed the principal components of the simulations. With initialisation, the prediction systems enhance the first leading mode which is the ENSO developing mode of the EASM. We further analysed the interaction between the EASM and ENSO (EASM-ENSO coupled mode) in both non-initialised and initialised simulations. The different depiction of EASM-ENSO coupled mode in the systems can explain their different response to the initialisation.

This is the logic and structure of the manuscript. We think that the reader can easily follow it.

Comment: The methods section has to be considerably improved. My biggest concern is that the results remain unclear to the point that it is difficult to judge if the paper is worthy of publication. It is e.g. unclear which start dates are used for the models, and if the study compares different start dates to each other, which would render the results not comparable and mostly useless.

Answer: We re-wrote the section 2.1. It gives a clearer information about the models and the analysed data.

We pointed out the study time period is 1979-2005 in both abstract (line 12) and section 2.1 (models and initialisation; line 87-104). As mentioned in section 2.1, the prediction systems employ different initialisation strategies, we selected the following months (up to 12 months) of each simulation for further analysis. It is easy to evaluate the seasonal prediction skill of the prediction systems under their initialisation strategy. Our findings indicate that, under current initialisation strategy, the GFDL-CM2p1 and the MIROC5 can be used for further seasonal prediction study of EASM.

Comment: The paper often reads more like a thesis than a paper. It should be made sure to explain the terms only where the reader cannot be assumed to know them, and the methods should be much more clearly explained. Throughout the paper, several paragraphs are misplaced and should be moved to a different section – e.g. the summary should not introduce new figures, and the results should not have to introduce new methods. The summary could be better structured. The English has to be improved – in several places it is difficult to understand what the authors mean.

Answer: Thanks for this useful comment. We changed the structure of the manuscript.
1) The introduction/selection of EASM index and the calculation of ENSO index have been moved to section 2.3 (EAST ASIAN MONSOON INDEX AND ENSO INDEX);
2) We added two figures, Figure 1 shows the predictability of six variables in the multi-model ensemble mean for both non-initialised and initialised experiment, and Figure 4 presents the observed first lead EOF mode of the six variables;
3) We deleted the citation of figures in summary;
4) We improved the English through the manuscript.

Detailed Comments:

Comment Line 9: sub-seasonal predictability is never mentioned again in the paper, probably better to leave it out in the abstract

Answer: Revised, line 9.

Comment Line 15: the zonal wind where?

Answer: Revised the sentence to *"We found that most prediction systems simulated zonal wind over 850 and 200 hPa were significantly improved in the initialised simulations …."*, line15-16.

Comment Lines 15/16 and 19 – 21 seem to contradict each other, please clarify

Answer: Revised the sentence.

Comment Line 25: to predict -> change to: of predicting

Answer: Done, line 27.

Comment Line 25: initialization of what?

Answer: changed the sentence to *"...predicting the EASM on a seasonal time-scale under the current initialisation strategy."* Line 27.

Comment Line 32: residents -> people

Answer: Done, line 34.

Comment Line 33: South Asian monsoon-SAM is confusing, I would suggest writing ". . .submonsoon systems, the South Asian monsoon (SAM) and the East Asian monsoon (EAM) (Wang. . .).

Answer: Done, line 35-36.

Comment Line 37: improve English: . . .predictions. . . is. . .

Answer: Revised, line 39.

Comment Line 41: how so?

Answer: We added one sentence to clarify it, *"This method establishes an empirical equation between the EASM and climate index…."* Line 44.

Comment Line 44/45: there are not really two kinds of climate models, it should be described as some being atmosphere-only with surface forcing, with the others including an ocean, while the atmosphere model stays the same. The reader does not need 10 lines of explanation of what the difference between an AGCM and an AOGCM is.

Answer: we modified these sentence to:

"Without initialisation, both the atmosphere general circulation models (AGCMs) and coupled atmosphere-ocean general circulation models (CGCMs) cannot predict the climate on seasonal time-scale (Goddard et al., 2001). Given initial condition, the AGCMs have ability to predict the climate, but show low skill in predicting the EASM (Wang et al., 2005;Barnston et al., 2010). Because the AGCMs fail to produce the correctly relationship between the EASM and sea surface temperature (SST) anomalies over the tropical western North Pacific, the South China Sea, and the Bay of Bengal (Wang et al., 2004;Wang et al., 2005). Therefore, the monsoon community endeavours to

predict the EASM with CGCMs (Wang et al., 2008a;Zhou et al., 2009;Kim et al., 2012;Jiang et al., 2013)." Line 47-56.

Comment Line 59: SST where?

Answer: Changed this sentence to *"...depends on their ability to reproduce the air-sea coupled process (Kug et al., 2008) and the given initial condition (Wang et al., 2005)." Line 59-61.*

Comment Line 60: initialization of what?

Answer: Changed this sentence to *"...depends on their ability to reproduce the air-sea coupled process (Kug et al., 2008) and the given initial condition (Wang et al., 2005)." Line 59-61*

Comment Line 69: what is an SST indicator?

Answer: Revised it to *"... SST variation index (i.e., El Niño-Southern Oscillation-ENSO index)...". Line 70-71*

Comment Line 75: improve English

Answer: Revised the sentence to *"2. Can the CMIP5 models capture the dynamical link between the ENSO and EASM?" Line 76*

Comment Lines 88 – 89: why do only these systems provide data? how were the runs obtained? How about the entire CHFP database? Are these used or was there a different source? CHFP would also include consistent start dates.

Answer: This study assesses the seasonal prediction skill of EASM in CMIP5 models. The six models provide yearly initialised simulations. The other CMIP5 models only provide 5-years initialised simulations. These models cannot be used for seasonal prediction study. The detailed description about the CMIP5 experiment can be found at Earth System Grid Federation (ESGF), *Taylor et al.,* (2012) and *Meehl et al.* (2014).

Comment Line 89: it is never mentioned which start dates are used here, it is only stated that several start dates exist for some of the models. Are you comparing the same start dates for all models? It does not seem so from the available data. Unfortunately, the table does not clarify this either. If different start dates are used, the comparison is likely useless and would have to be repeated with consistent start dates.

Answer: We revised the expression of the section 2.1 (models and initialisation).

Following the prediction framework of CMIP5, the six prediction systems established their initialisation strategy. There is a little bit difference of initialisation strategy between the six prediction systems (Table 2 and section 2.1). The reference papers in Table 1 show that the six systems have ability to predict the global climate with the current initialisation strategy. Intercomparison the six models can conclude the useful initialisation strategy for seasonal prediction of the EASM. In fact, our finding indicates that the GFDL-CM2p1 and the MIROC5 can be used for further seasonal prediction study of the EASM with the current initial strategy. Therefore, we think that the hypothesis of the paper is correct.

Comment Line 89: What does un-initialized mean? Are the "uninitialized" runs computed for a certain time frame?

Answer: We added some sentences to explain it. Line 90-93

"For non-initialised simulations, the models were forced by observed atmospheric composition changes (reflecting both anthropogenic and natural sources) and, for the first time, including the time-evolving land cover (Taylor et al., 2012)."

Comment Line 91: "on each pre-year 1st November": improve English

Answer: We added the initialised date for each model in Table 2.

Comment Line 98: change to: The configurations of the six prediction systems are summarized in Table 2.

Answer: Done.

Comment Line 114-116: how about comparing the mean state in the models first before having to include the mean state in the PCC? That would make things simpler and clearer.

Answer: We added a figure to show the predictable area of multi-model ensemble mean in both non-initialised and initialised experiment. Now it makes things easy to follow.

Comment Lines 118 – 120: this is not clear, improve English

Answer: Sentences have been improved.

Comment Lines 130 – 140: a bit lengthy

Answer: Paragraph has been reformulated and shortened.

Comment Line 158: I don't understand this sentence

Answer: We changed the sentence to *"These variables have been widely used to calculate monsoon index (Wang et al., 2008b)." line 183-184*

Comment Lines 168. . .: this should not be a part of the results, this should come earlier

Answer: The paragraph has been moved to section 2.3. Line 114-132

Comment Lines 180-182: which season is depicted here? This will be crucial for understanding what the paper is trying to say

Answer: The paper is talking about seasonal prediction of the EASM. This sentence shows clearly as *"In non-initialised simulations, none of the models captures the observed EASM, as indicated by an insignificant ACC (Figure 3)." Line 200-201*

Then, in section 2.3, there is a sentence to clarify the monsoon index *"The June-July-August mean of WF-index is used to represent the EASM for further analysis in this study." Line 126-127*

Comment Line 191: unfortunately I don't know what a sandwich pattern is supposed to look like. Since these EOFs are talked about so much here, they should be shown in a figure. It should be made clear why it helps to compute EOFs for predictability.

Answer: We added Figure 4 to show the observed first leading EOF model of monsoon precipitation and general circulation, and the associated principal component.

Comment Lines 203/206: what is ua? Zonal wind anomaly? Anomaly with respect to what?

Answer: In table 3, there is a sentence to explain *"The abbreviation of the variables is followed to the guidelines of CMIP5."* More details can be found at http://cmip-pcmdi.llnl.gov/cmip5/docs/standard_output.pdf

Comment Line 229: this should be part of the methods

Answer: It has been moved to section 2.3.

Comment Line 235: I don't see this in Fig. 5

Answer: Revised.

Comment Line 239: when is it initialized?

Answer: Changed it to *"...in initialised experiments." Line 250*

Comment Line 245: why is the correlation between Nino3.4 and the SOI important for predictability of the monsoon? Explain!

Answer: We revised the sentence (line 259-262). There is a short discussion about the correlation between Niño3.4 and the SOI in Section 5 (line 287-296).

Comment Line 263: how is that defined? Which months are used?

Answer: Figure 8 shows clearly that the lead-lag correlation coefficients between the EASM index and ENSO indices. This is defined as the ESNO-EASM coupled mode in previous monsoon studies. Here, we take this definition and analyse it in the simulations. As we mentioned, the EASM index is defined as the summer season (June-July-August; JJA) mean of monsoon index. The seasonal mean of ENSO indices (Niño3.4, and SOI) is applied to calculate the lead-lag correlation.

Comment Line 294: so why exactly is there an improvement from non-initialized to initialized models?

Answer: In section 5 (Discussion), we made a short discussion about the relationship between Niño3.4 and the SOI represented in non-initialised and initialised simulations.

"The change of the correlation between Niño3.4 and the SOI is insignificant from non-initialised to initialised simulations. We therefore conclude that the relationship between Niño3.4 and the SOI depends more on the model parameterisation than on the initial condition." Line 298-302.

Comment Line 301: you cannot introduce a new figure in the summary. This should be part of the results

Answer: You are right. We deleted the citation of figure in the summary.

Comment Line 317: this should come much earlier

Answer: The initialisation strategies are present in Table 2. Here, we mention it to discuss how the models work with the given initial condition. Line 287-289

Comment Line 358: what are the IRI models?

Answer: We added four sentences to explain the IRI models and discuss their limitation for EASM prediction. The four sentences as:

"There are 4 AGCMs contributing to the IRI prediction system, including ECHAM4.5, CCM3.6, COLA and GFDL-AM2p14. These models are forced by prescribed SST to

forecast the climate on seasonal time-scale. Barnston et al. (2010) found that the models show low prediction skill over East Asia. Therefore, the IRI prediction system cannot be used to predict the EASM." Line 328-332

Comment Line 359: most of the models used here are seasonal forecast models already, not sure what you are trying to say

Answer: Exactly, the two models (ECMWF System and the NCEP CFS) have been developed as seasonal forecast system. However, both the two systems show low prediction skill of EASM (Jiang et al., 2013; Kim et al., 2012). The CMIP5 models demonstrate a comparable prediction skill of EASM as the two seasonal forecast systems. Therefore, the CMIP5 models have potential to be developed as application system for EASM seasonal prediction, especially the GFDL-CM2p1 and the MIROC5.

Comment Line 365: SST where?

Answer: As we discussed in Line 303-325, the prediction systems cannot represent the second EOF lead mode which is the Indo-western Pacific monsoon-ocean coupled mode even given initial condition. Therefore, the prediction skill of EASM might can be improved while the systems optimise the SST-EASM interaction.

Comment Figure 3: should be better explained in the main text

Answer: There is a paragraph to describe the figure, line 213-227

1   Seasonal Prediction Skill of East Asian Summer Monsoon in CMIP5-Models

2   *Bo Huang,* Ulrich Cubasch, Christopher Kadow*

3   *Institute of Meteorology, Freie Universität Berlin,*
4   *Carl-Heinrich-Becker-Weg 6-10, 12165 Berlin, Germany*

5   *Email: huangb@zedat.fu-berlin.de*

6

7   **ABSTRACT**

8   The East Asian summer monsoon (EASM) is an important part of the global climate system

9   and plays a vital role in the Asian climate. Its seasonal predictability is a long-standing issue

10   within the monsoon scientist community. In this study, we will analyse the seasonal (the

11   leading time is at least six months) prediction skill of the EASM rainfall and its associated

12   general circulation in non-initialised and initialised simulations for the years 1979-2005

13   which were performed by six prediction systems (*i.e.*, the BCC-CSM1-1, the CanCM4, the

14   GFDL-CM2p1, the HadCM3, the MIROC5 and the MPI-ESM-LR) from the Coupled Model

15   Intercomparison Project phase 5 (CMIP 5). We found that most prediction systems simulated

16   zonal wind over 850 and 200 hPa were significantly improved in the initialised simulations

17   compared to non-initialised simulations. Based on the knowledge that zonal wind indices can

18   be used as potential predictors for the EASM, we selected an EASM index based upon the

19   zonal wind over 850 hPa for further analysis. This assessment showed that the GFDL-CM2p1

20   and the MIROC5 added prediction skill in simulating the EASM index with initialisation, the

21   BCC-CSM1-1, the CanCM4, and the MPI-ESM-LR changed the skill insignificantly, and the

22   HadCM3 indicated a decreased skill score. The different response to the initialisation can be

23   traced back to the ability of the models to capture the ENSO (El Niño-Southern Oscillation)-

24   EASM coupled mode, particularly the Southern Oscillation-EASM coupled mode. As it is

25   known from observational studies, this mode links the oceanic circulation and the EASM

26   rainfall. On the whole, we find that the GFDL-CM2p1 and the MIROC5 are capable of

27   predicting the EASM on a seasonal time-scale under the current initialisation strategy.

28   **Key Words**: East Asian summer monsoon; initialisation; seasonal prediction; ENSO-EASM

29   coupled mode; CMIP5

Commented [BH1]: Detailed comment (DC) 1

Commented [BH2]: Detailed comment 2 and 3

Commented [BH3]: Detailed comment 4

Commented [BH4]: Detailed comment 5

1. INTRODUCTION

The Asian monsoon is the most powerful monsoon system in the world due to the thermal contrast between the Eurasian continent and the Indo-Pacific Ocean. Its evolution and variability critically influences the livelihood and the socio-economic status of over two billion people who live in the Asian monsoon dominated region. It encompasses two sub-monsoon systems, the South Asian monsoon (SAM) and the East Asian monsoon (EAM) (Wang, 2006). In summer time (June-July-August), the EAM, namely, the East Asian summer monsoon (EASM) occurs from the Indo-China peninsula to the Korean Peninsula and Japan, and shows strong intraseasonal-to-interdecadal variability (Ding and Chan, 2005). Thus, an accurate prediction of the EASM is an important and long-standing issue in climate science.

To predict the EASM, there are two approaches, a statistical prediction and a dynamical prediction, respectively. The statistical method seeks the relationship between the EASM and a strong climate signal (e.g., ENSO, NAO; Wu et al., 2009;Yim et al., 2014;Wang et al., 2015). This method establishes an empirical equation between the EASM and climate index. However, it is limited by the strength of the climate signal. The other method is a dynamical prediction. It employs a climate model to predict the EASM (Sperber et al., 2001;Kang and Yoo, 2006;Wang et al., 2008a;Yang et al., 2008;Lee et al., 2010;Kim et al., 2012). Without initialisation, both the atmosphere general circulation models (AGCMs) and the coupled atmosphere-ocean general circulation models (CGCMs) cannot predict the climate on a seasonal time-scale (Goddard et al., 2001). Given an initial condition, the AGCMs have the ability to predict the climate, but show little kill in predicting the EASM (Wang et al., 2005;Barnston et al., 2010). Because the AGCMs fail to produce a correct relationship between the EASM and the sea surface temperature (SST) anomalies over the tropical western North Pacific, the South China Sea, and the Bay of Bengal (Wang et al., 2004;Wang et al., 2005). Therefore, the monsoon community endeavours to predict the EASM with CGCMs (Wang et al., 2008a;Zhou et al., 2009;Kim et al., 2012;Jiang et al., 2013).

CGCMs have proved to be the most valuable tools in predicting the EASM (Wang et al., 2008a;Zhou et al., 2009;Kim et al., 2012;Jiang et al., 2013). However, the performance of CGCMs in predicting the EASM on seasonal time-scale strongly depends on their ability to reproduce the air-sea coupled process (Kug et al., 2008) and the given initial condition (Wang et al., 2005). In the coupled model inter-comparison project (CMIP) phase 3 (CMIP3; Meehl

2

Commented [BH5]: Detailed comment 6

Commented [BH6]: Detailed comment 7

Commented [BH7]: Detailed comment 8

Commented [BH8]: Detailed comment 9

Commented [BH9]: Detailed comment 10

Commented [BH10]: Detailed comment 11 and 12

62 et al., 2007) era, the models simulate, not only a too weak tropical SST-monsoon
63 teleconnection (Kim et al., 2008;Kim et al., 2011), but also a too weak East Asian zonal
64 wind-rainfall teleconnection (Sperber et al., 2013). Compared to CMIP3 models, CMIP phase
65 5 (CMIP5; Taylor et al., 2012) models improved the representation of monsoon status
66 (Sperber et al., 2013). Therefore, given the initial conditions, the CMIP5 models do have the
67 potential to predict the EASM.

68 As mentioned, initial conditions do play a vital factor in predicting the EASM on sub-
69 seasonal to seasonal time-scale (Wang et al., 2005;Kang and Shukla, 2006). Under the
70 current set up of initialisation, the CMIP5 models showed the ability to predict the SST
71 variation index (*i.e.,* El Niño-Southern Oscillation-ENSO index) of up to 15 months in
72 advance (Meehl and Teng, 2012;Meehl et al., 2014;Choi et al., 2016). This extended
73 prediction skill of the ENSO suggests that the EASM can be predicted on a seasonal time-
74 scale if the dynamical link between the ENSO and monsoon circulations is well represented
75 in these models. Two scientific questions will be addressed in this study: 1. How realistic are
76 the initialised CMIP5 models in representing the EASM? 2. Can the CMIP5 models capture
77 the dynamical link between the ENSO and EASM?

Commented [BH11]: Detailed comment 13

Commented [BH12]: Detailed comment 14

78 In this paper, we will intercompare the influence of the initialisation on the capability of
79 the CMIP5 model to capture the EASM and the ENSO-EASM teleconnections. The model
80 simulations, comparison data and methods are introduced in Section 2. Section 3 describes
81 the seasonal skill of the rainfall predictions and the prediction of the associated general
82 circulation of the EASM. The mechanism causing the differential response of the models to
83 the initialisation is presented in Section 4. The discussions are shown in Section 5. Section 6
84 summarises the findings of this paper.

85 **2.   MODELS, DATA AND METHODS**
86 **2.1 MODELS AND INITIALISATION**
87 In this study, we assessed six prediction systems from CMIP5 project (Table 1). The six
88 prediction systems have performed a yearly initialisation (Meehl et al., 2014). Their
89 simulations can be used in seasonal prediction study. There are two group of experiments,
90 without initialisation (non-initialisation) and with initialisation, respectively. For non-
91 initialised simulations, the models were forced by observed atmospheric composition changes
92 (reflecting both anthropogenic and natural sources) and, for the first time, including the time-
93 evolving land cover (Taylor et al., 2012). For initialised simulations, the models update the

Commented [BH13]: Detailed comment 17

3

time-evolving observed atmospheric and oceanic component (Taylor et al., 2012). Following the CMIP5 framework, the six models established their initialisation strategy, which are summarised in Table 2. More details about the initialisation strategy of each model can be found in the reference paper in Table 1. To simplify the comparison, we select the first lead year (up to 12 months) results for further analysis. The HadCM3-ff is the full-field initialised simulation, which employs the same CGCM (HadCM3) as the anomaly initialisation. We select the satellite era (1979 to 2005) for our study due to the spatial coverage of precipitation observations.

2.2 COMPARISON DATA

The main datasets which were used for comparison in this study include: (1) monthly precipitation data from the Global Precipitation Climatology Project (GPCP; Adler et al., 2003); (2) monthly circulation data from ECMWF Interim re-analysis (ERA-Interim; Dee et al., 2011); and (3) monthly mean SST from National Oceanic and Atmospheric Administration (NOAA) improved Extended Reconstructed SST version 4 (ERSST v4; Huang et al., 2015). All the model data and the comparison data are remapped onto a common grid of 2.5º×2.5º by bi-linear interpolation to reduce the uncertainty induced by different data resolutions.

2.3 EAST ASIAN MONSOON INDEX AND ENSO INDEX

In recent decades, more than 25 general circulation indices have been produced to define the variability and the long-term change of the EASM. Wang et al. (2008b) arranged them according to their ability to capture the main features of the EASM. They found that the Wang and Fan index (hereafter WF-index; 1999) showed the best performance in capturing the total variance of the precipitation and three-dimensional circulation over East Asia. We, thus, select the WF-index for further analysis. Its definition is a standardised average zonal wind at 850 hPa in (5°-15ºN, 90°-130ºE) minus in (22.5°-32.5ºN, 110°-140ºE). The WF-index is a shear vorticity index which often is described by a north-south gradient of the zonal winds. In positive (negative) phase of the WF-index years, two strong (weak) rainfall belts located at the Indo China Peninsula-to-the Philippine Sea and the northern China-to-the Japanese Sea, and a weak (strong) rainfall belt occurs from the Yangtze river basin-to-the south of Japan. The June-July-August mean of WF-index is used to represent the EASM for further analysis in this study.

4

125   Here, we choose the Niño3.4 and southern oscillation index (SOI) to represents the
126 ENSO status. The Niño3.4 is calculated by the SST anomaly in the central Pacific (190-
127 240ºE, 5ºS-5ºN), while the SOI is based upon the anomaly of the sea level pressure
128 differences between Tahiti (210.75ºE, 17.6ºS) and Darwin (130.83ºE, 12.5ºS). To calculate
129 the SOI, we interpolate the grid data to the Tahiti and the Darwin point by bilinear
130 interpolation.

131 **2.4 METHODS**

132   In this study, we chose the un-centred Pattern Correlation Coefficient (PCC) (for more
133 details see Barnett and Schlesinger, 1987) to analyse the model performance in comparison to
134 the observational data, because centred correlations alone are not sufficient for the attribution
135 of seasonal prediction (Mitchell et al., 2001). The un-centred PCC is defined by:

$$PCC = \frac{\sum_{x=1}^{n} \sum_{y=1}^{m} w_{(x,y)} F_{(x,y)} A_{(x,y)}}{\sqrt{\sum_{x=1}^{n} \sum_{y=1}^{m} w_{(x,y)} F_{(x,y)}^2 \sum_{x=1}^{n} \sum_{y=1}^{m} w_{(x,y)} A_{(x,y)}^2}}$$

136

137 where n and m are grids on longitude and latitude, respectively. $F_{(x,y)}$ and $A_{(x,y)}$ represent two
138 dimensions comparison and validating value. $w_{(x,y)}$ indicates the weighting coefficient for
139 each grid. An equal weighting coefficient was applied due to the study area in East Asia
140 where we can omit the convergence of the longitudes with the latitudes.

141   We also employed the anomaly correlation coefficient (ACC) to analyse the model
142 performance in reproducing observational variations. The ACC is the correlation between
143 anomalies of forecasts and those of verifying values with the reference values, such as
144 climatological values (Drosdowsky and Zhang, 2003). Its definition is:

$$ACC = \frac{\sum_{i=1}^{n} w_i (f_i - \bar{f})(a_i - \bar{a})}{\sqrt{\sum_{i=1}^{n} w_i (f_i - \bar{f})^2 \sum_{i=1}^{n} w_i (a_i - \bar{a})^2}}, (-1 \leq ACC \leq 1)$$

145

$$f_i = F_i - C_i, \bar{f} = \left(\sum_{i=1}^{n} w_i f_i\right) \Big/ \sum_{i=1}^{n} w_i$$

146

$$a_i = A_i - C_i, \bar{a} = \left(\sum_{i=1}^{n} w_i a_i\right) \Big/ \sum_{i=1}^{n} w_i$$

147

5

where n is the number of samples, and F_i, A_i, C_i represent comparison, verifying value, and reference value such as climatological value, respectively. Also, $\overline{f}$ is the mean of f_i, $\overline{a}$ is the mean of a_i, and w_i indicates the weighting coefficient. If the variation of anomalies of comparison dataset is a coincident with that of the anomalies of verifying value, ACC will take 1 (the maximum value). Otherwise, if the variation is completely reversed, ACC is -1 (the minimum value).

Commented [BH20]: Detailed comment 22

The root-mean-square-error (RMSE) is employed to check the model deviation from the observation and its definition is:

$$RMSE = \sqrt{\sum_{i=1}^{n} w_i D_i^2} \bigg/ \sqrt{\sum_{i=1}^{n} w_i}$$

where D_i represents the deviation between comparison and verifying value, w_i is the weighting coefficient for each sample, and n is the number of samples. If RMSE is closer to zero, it means that the comparisons are closer to the verifying values.

3. SEASONAL PREDICTION SKILL OF THE EASM

The EASM has complex spatial and temporal structures that encompass the tropics, subtropics, and midlatitudes (Tao and Chen, 1987;Ding, 1994). In the late spring, an enhanced rainfall pattern was observed in the Indochina Peninsula and in the South China Sea. At the same time, the rainfall belt advances northwards to the south of China. In the early summer, the rainfall concentration occurred in the Yangtze River Basin and in southern Japan, namely, the Meiyu and Baiu seasons, respectively. The rainfall belt can reach as far as northern China, the Korean Peninsula (called the Changma rainy season) and central Japan in July (Ding, 2004;Ding and Chan, 2005).

The EASM is characterised by both seasonal heterogeneous rainfall distribution and associated large-scale circulation systems (Wang et al., 2008b). In the summer season, water moisture migrates from the Pacific Ocean to central and eastern Asia, which is carried by the southwest surface winds. Generally, a strong summer monsoon year is followed by precipitation in northern China, while a weak summer monsoon year is usually accompanied by heavier rainfall along the Yangtze River basin (Ding, 1994;Zhou and Yu, 2005).

6

175 For multi-model ensemble mean (MME), the prediction skill of the June-July-August
176 mean rainfall and the associated general circulation variable (*i.e.*, zonal and meridional wind,
177 and mean sea level pressure) is presented in Figure 1. These variables have been widely used
178 to calculate the monsoon index (Wang et al., 2008b). Table 3 shows the contribution of these
179 variables in the EASM. Their abbreviations follow the guidelines of CMIP5 (Taylor et al.,
180 2012). Compared to the non-initialised experiment, a larger predicted area can be found in the
181 initialised experiment, especially for the psl, ua850 and ua200. There are small changes to the
182 predicted area between the non-initialised and initialised experiment for the pr, va850 and
183 va200. The individual model shows an acceptable performance (high PCC) in capturing the
184 observed spatial variation of the six variables, but a poor performance in simulating their
185 temporal variation (with low ACC) (Figure 2). There is no improvement in estimating the
186 spatial variation of the six variables with initialisation. We can see that the models show a
187 higher ACC in the initialised simulations than that in the non-initialised ones. The
188 improvement of simulating the temporal variation of zonal winds (*i.e.*, ua850 and ua200) is
189 larger than that of the rainfall and meridional winds. One can exploit this improvement by
190 using a general circulation based monsoon index as a tool to predict the EASM. As
191 mentioned in section 2.3, the WF-index better represents the monsoon rainfall and its
192 associated general circulation structure than the other monsoon index. Therefore, the
193 prediction skill of EASM in the following analysis is based on the WF-index.

194 In non-initialised simulations, none of the models captured the observed EASM, as
195 indicated by an insignificant ACC (Figure 3). The CanCM4 and the GFDL-CM2p1 simulate
196 a negative phase, while the BCC-CSM1-1, the HadCM3, the MIROC5 and the MPI-ESM-LR
197 all predicted a positive phase of the EASM. With initialisation, the GFDL-CM2p1 and the
198 MIROC5 improved the skill to simulate the EASM, the CanCM4 and the MPI-ESM-LR
199 displayed hardly any reaction, while the BCC-CSM1-1 and the HadCM3 showed a worse
200 performance than without initialisation. Particularly with anomaly initialisation, the HadCM3
201 significantly lost its prediction skill in capturing the EASM. The CMIP5 models showed
202 different response to the initialisation in predicting the EASM on seasonal time-scale. To
203 understand the potential reason, we analysed the principle components of six variables, which
204 contributed to the EASM. The details are presented in Section 4.

Commented [BH21]: Detailed comment 23

Commented [BH22]: Detailed comment 25

4. EASM-ENSO COUPLED MODE IN CMIP5

We employed the EOF method to analyse the leading EOF modes of the six meteorological variables anomaly in the EASM region (0°-50ºN, 100°-140ºE). The first EOF mode of the rainfall is characterised by a "sandwich" pattern, which showed sharp contrast between the prominent rainfall centre over Malaysia, the Yangtze River valley and the south of Japan, and the enhanced rainfall over the Indo-China Peninsula and the Philippine Sea (Figure 4). The increased precipitation is associated with cyclones in the low-level (850 hPa) and anti-cyclones in the upper level (200 hPa).

The correlation coefficient of the first eigenvector and the associated principal component (PC) between the model simulation and the observation in the non-initialised and the initialised simulation is presented in Figure 5. The models captured the eigenvector of the first EOF for the six meteorological fields in non-initialised simulation. However, they failed to reproduce the associated PC of the first leading EOF mode. Compared to the non-initialised simulation, the models showed no improvement to simulate the first leading EOF mode of rainfall, but exhibit a better performance in representing the first leading EOF mode of zonal wind. The CanCM4 and the GFDL-CM2p1 captured the first PC of ua850, but not the other five models. For the zonal wind at 200 hPa, the BCC-CSM1-1 fails to simulate its first EOF mode while the other six models can. Only the GFDL-CM2p1 accurately simulates the first EOF eigenvectors and the associated PC of va850, which cannot be reproduced in the other models. No models captured the spatial-temporal variation of the first EOF mode of meridional wind at 200 hPa. In addition, the GFDL-CM2p1 and the MIROC5 simulates a reasonable leading EOF mode and associated PC of psl, while the other models do not capture it.

Figure 6 shows the fractional (percentage) variances of the six variables from the first EOF mode with the total variances from the observation, and the model simulation with (with-out) initialisation. The observational total variances for the pr, the ua850, the ua200, the va850, the va200 and the psl, are depicted by the first lead EOF mode in 21.2, 59.0, 36.5, 20.6, 28.5 and 50.0 percent, respectively. The models simulated the comparable explanatory variances, which showed a slight discrepancy for the first leading mode in the non-initialisation. From non-initialised simulation to initialised simulation, the CGCMs tended to enhance the first EOF leading mode because they show larger fractional variances of the total

8

Commented [BH23]: Detailed comment 4

Commented [BH24]: Detailed comment 39

236 variances of the six variables. We note that the CanCM4 and the GFDL-CM2p1 significantly

237 increased the fractional variances from non-initialisation to initialisation.

238   The ENSO is a dominant mode of the inter-annual variability of the coupled ocean and

239 atmosphere climate system, which has strong effects on the inter-annual variation of the

240 EASM (Wang et al., 2000;Wu et al., 2003). Wang et al. (2015) summarised that the first EOF

241 lead mode of the ASM is ENSO developing mode. As previously mentioned, the first EOF

242 mode was improved in the initialised simulations, compared to the non-initialised simulation.

243 This also can be found in the ENSO indices (Figure 7). The individual members and their

244 ensemble mean of the six models show a low correlation coefficient to the observational

245 Niño3.4 and the SOI in the non-initialised simulations. These two indices showed strong anti-

246 phases in the observation, with the correlation range being -0.94 to -0.92 for four seasons

247 (DJF, MAM, JJA, SON). Without initialisation, the models can describe the anti-correlation

248 between Niño3.4 and the SOI, but with weaker correlation. Compared to the non-

249 initialisation, there is a significant improvement for models in capturing the observational

250 Niño3.4 and the SOI in the initialised experiments. The initialisation lowers the spread of

251 Niño3.4 and the SOI in all the six models. There is a noticeable change between the model in

252 producing the relationship between the Niño3.4 and the SOI. We found that the GFDL-

253 CM2p1 (HadCM3) shows a lower (higher) Niño3.4-SOI correlation in initialisation than that

254 in non-initialisation. With initialisation, the ensemble mean of each model outperforms its

255 individual members in capturing Niño3.4 and the SOI, while without initialisation it showed

256 a worse performance than that of the individual members in simulating Niño3.4 and the SOI.

257   The EASM strongly relies on the pre-seasons ENSO signal due to the lag response of

258 the atmosphere to the SST anomaly (Wu et al., 2003). The lead-lag correlation coefficients

259 between the EASM index and the Niño3.4, and the SOI from JJA(-1) to JJA(+1) are

260 illustrated in Figure 8. The pre-season Niño3.4 (SOI) presents a significant negative

261 (positive) correlation to the EASM, while the post-season Niño3.4 (SOI) showed a notable

262 positive (negative) correlation. This lead-lag correlation coefficient phase is called the

263 Niño3.4-/SOI-EASM coupled mode (Wang et al., 2008b). In the non-initialised cases, the

264 models do not produce the teleconnection between the ENSO and the EASM. The CanCM4,

265 the HadCM3 and the MPI-ESM-LR failed to represent the lead-lag correlation coefficient

266 differences between pre-/post-season ENSO and EASM. The BCC-CSM1-1, the GFDL-

267 CM2p1 and the MIROC5 captured the coupled mode of the ENSO and the EASM. However,

9

the pre-season ENSO has a weak effect on the EASM. Compared to the non-initialised cases, the MIROC5 and the GFDL-CM2p1 both demonstrated a significant improvement in simulating Niño3.4 (SOI)-EASM coupled mode in the initialisation. The BCC-CSM1-1, the HadCM3, and the HadCM3-ff showed no improvement, with insignificant correlation between Niño3.4 (SOI) and the EASM. The CanCM4 and the MPI-ESM-LR indicated a higher correlation between the EASM and the simultaneous-to-post-season ENSO than to the pre-season ENSO.

5. DISCUSSION

The model exhibits a better performance in simulating the general circulation of the EASM with initialisation. Thus, initialisation is helpful in forecasting the EASM on a seasonal time-scale. There are two initialisation methods in our study, full-field initialisation and anomaly initialisation (Table 1). The full-field initialisation produces more skilful predictions on the seasonal time-scale in predicting regional temperature and precipitation (Magnusson et al., 2013; Smith et al., 2013). Nevertheless, for predicting the EASM, there is no significant difference between the two methods. We can see that both the GFDL-CM2p1 and the MIROC5 have a significant improvement in capturing the EASM, with full-field and anomaly initialisation, respectively. Only the HadCM3 was initialised by the two initialisation techniques. However, both these two initialised techniques are producing poor predictions of the EASM with no major differences.

The current initialisation strategy updates the observed atmospheric component (*i.e.*, zonal and meridional wind, geopotential height, *etc*.) and the SST (Meehl et al., 2009; Taylor et al., 2012; Meehl et al., 2014). With initialisation, the SST conveys its information via the large heat content of the ocean to the coupled system. Therefore, an index indicating an ocean oscillation like Niño3.4 showed a seasonal-to-decadal prediction skill (Jin et al., 2008; Luo et al., 2008; Choi et al., 2016). The models studied here demonstrated a prediction skill in simulating Niño3.4 and the SOI due to this effect. The change of the correlation between Niño3.4 and the SOI is insignificant from non-initialised to initialised simulations. We therefore conclude that the relationship between Niño3.4 and the SOI depends more on the model parameterisation than on the initial condition.

Wang *et al*. (2015) found that the second EOF mode of ASM is the Indo-western Pacific monsoon-ocean coupled mode, the third is the Indian Ocean dipole (IOD) mode, and the fourth is the trend mode. The Indo-western Pacific monsoon-ocean coupled mode is the

10

Commented [BH27]: Detailed comment 35

Commented [BH28]: Detailed comment 31

Commented [BH29]: Detailed comment 33

atmosphere-ocean interaction mode (Wang et al., 2013;Xiang et al., 2013), which is supported by a positive thermodynamic feedback between the western North Pacific (WNP) anticyclone and the underlying Indo-Pacific sea surface temperature anomaly dipole over the warm pool (Wang et al., 2015). The IOD increases the precipitation from the South Asian subcontinent to southeastern China and suppresses the precipitation over the WNP (Wang et al., 2015). It affects the Asian monsoon by the meridional asymmetry of the monsoonal easterly shear during the boreal summer, which can particularly strengthen the northern branch of the Rossby wave response to the south-eastern Indian Ocean SST cooling, leading to an intensified monsoon flow as well as an intensified convection (Wang and Xie, 1996;Wang et al., 2003;Xiang et al., 2011;Wang et al., 2015). We noted that the models simulate a reasonable first EOF mode, but illustrate no skill in capturing the other EOF leading modes (not shown). We argue that the models cannot well represent the monsoon-ocean interaction, even with initialisation. The models do not simulate the third EOF leading mode of the EASM since the predictability of the IOD extends only over a three-month time-scale (Choudhury et al., 2015). The current initialisation strategies (both anomaly and full field) enhance the ENSO signal in the model simulations with higher explained fraction of variance. Kim et al. (2012) described a similar finding in ECMWF System 4 and NCEP Climate Forecast System version 2 (CFSv2) seasonal prediction simulations. With initialisation, the models well predict ENSO on seasonal time-scale, which leads to an overly strong modulation of the EASM by ENSO (Jin et al., 2008;Kim et al., 2012).

> **Commented [BH30]:** Detailed comment 38

It is worth mentioning that it was an extremely weak monsoon and strong El Niño year in 1998. The CanCM4, the GFDL-CM2p1, the MIROC5 and the MPI-ESM-LR have the ability to simulate the extreme monsoon event, while the BCC-CSM1-1, and the HadCM3 do not capture it even with initialisation. There is the potential for the BCC-CSM and the HadCM models to improve the teleconnection between the ENSO and the EASM.

This study has discussed six CMIP5 models in predicting the EASM on seasonal time-scale. The six models are earth system coupled models which present a better SST-monsoon teleconnection than CMIP3 models (Sperber et al., 2013) and IRI (International Research Institute for Climate and Society) models (Barnston et al., 2010). There are 4 AGCMs contributing to the IRI prediction system, including ECHAM4.5, CCM3.6, COLA and GFDL-AM2p14. These models are forced to forecast the climate on seasonal time-scale by prescribed SST. Barnston et al. (2010) found that the models showed low prediction skill

11

over East Asia. Therefore, the IRI prediction system cannot be used to predict the EASM. There are two seasonal forecast application systems, the ECMWF System and the NCEP CFS, respectively. Both the two application systems have low prediction skill of EASM (Kim et al., 2012;Jiang et al., 2013). The CMIP5 models have potential to be developed as application system for EASM seasonal prediction, especially the GFDL-CM2p1 and the MIROC5.

We have compared six CMIP5 systems with their respective initialisation strategies. The GFDL-CM2p1 and the MIROC5 have the potential to serve as seasonal forecast application system even with their current initialisation method. These models have great potential to optimise the SST-EASM interaction simulation performance to improve their seasonal prediction skill of the EASM.

6.   SUMMARY

Six earth system models from CMIP5 have been selected in this study. We have analysed the improvement of the rainfall, the mean sea level pressure, the zonal wind and the meridional wind in the EASM region from non-initialisation to initialisation. The low prediction skill of the summer monsoon precipitation is due to the uncertainties of cloud physics and cumulus parameterisations in the models (Lee et al., 2010;Seo et al., 2015). The models showed a better performance in capturing the inter-annual variability of zonal wind than the precipitation after initialisation. Thus, the zonal wind index is an additional factor, which can indicate the prediction skill of the model. When, we calculate the WF-index in both non-initialised and initialised simulations, the GFDL-CM2p1 and the MIROC5 showed a significant advancement in simulating the EASM from non-initialised to initialised simulation with a lower RMSE and a higher ACC. There is only a slight change in the WF-index calculated from the BCC-CSM1-1, the CanCM4 and the MPI-ESM-LR data with initialisation. Compared to the non-initialised simulation, the HadCM3 loses prediction skill, especially with anomaly initialisation.

To test the possible mechanisms of the models' performance in the non-initialisation and the initialisation, we have calculated the leading mode of the six fields, which are associated to the EASM. The models demonstrated a better agreement with the observational first EOF mode in the initialised simulations. The first lead mode of zonal wind at 200 hPa showed a significant improvement in the models except the BCC-CSM1-1 with initialisation. Therefore, a potential predictor might be an index based upon the zonal wind at 200 hPa.

12

Compared to the non-initialisation, the models enhanced the first EOF mode with a higher fraction of variance to the total variance after initialisation. The first EOF mode of the EASM is the ENSO developing mode (Wang et al., 2015). We have analysed the seasonal simulating skill of Niño3.4 and the SOI in each model. The models showed a poor performance in representing Niño3.4 and the SOI in the non-initialised simulation. Initialisation improved the model simulating skill of Niño3.4 and the SOI. The initialised simulations decreased the spread of ensemble members in the models. We found that there is no significant change in the models reproducing the correlation between Niño3.4 and the SOI from non-initialisation to initialisation.

In general, the pre-season warm phase of the ENSO (El Niño) leads to a weak EASM producing more rainfall over the South China Sea and northwest China, and less rainfall over the Yangtze River Valley and the southern Japan; the cold phase of the ENSO (La Niña) illustrated a reverse rainfall pattern to El Niño in East Asia. The pre-season Niño3.4 (SOI) exhibits a strong negative (positive) correlation to the EASM, while the correlation between the post-season Niño3.4 (SOI) and the EASM illustrated an anti-phase as the pre-season. In the non-initialised simulations, the models do not capture Niño3.4-/SOI-EASM coupled mode. We found that only the MIROC5 has the ability to represent the Niño3.4-EASM coupled mode with initialisation. For the SOI-EASM coupled mode, the GFDL-CM2p1 and the MIROC5 captured it in the initialisation, while the BCC-CSM1-1, the HadCM3, the HadCM2-ff, the CanCM4 and the MPI-ESM-LR do not. Therefore, we argue that the differential depiction of ENSO-EASM coupled mode in CMIP5 models lead to their differential response to initialisation.

References

Adler, R. F., Huffman, G. J., Chang, A., Ferraro, R., Xie, P.-P., Janowiak, J., Rudolf, B., Schneider, U., Curtis, S., Bolvin, D., Gruber, A., Susskind, J., Arkin, P., and Nelkin, E.: The Version-2 Global Precipitation Climatology Project (GPCP) Monthly Precipitation Analysis

13

397 (1979–Present), J Hydrometeorol, 4, 1147-1167, 10.1175/1525-
398 7541(2003)004<1147:tvgpcp>2.0.co;2, 2003.
399 Arora, V. K., Scinocca, J. F., Boer, G. J., Christian, J. R., Denman, K. L., Flato, G. M.,
400 Kharin, V. V., Lee, W. G., and Merryfield, W. J.: Carbon emission limits required to satisfy
401 future representative concentration pathways of greenhouse gases, Geophys Res Lett, 38,
402 L05805, 10.1029/2010gl046270, 2011.
403 Barnett, T. P., and Schlesinger, M. E.: Detecting Changes in Global Climate Induced by
404 Greenhouse Gases, J Geophys Res Atmos, 92, 14772-14780, 10.1029/JD092iD12p14772,
405 1987.
406 Barnston, A. G., Li, S. H., Mason, S. J., DeWitt, D. G., Goddard, L., and Gong, X. F.:
407 Verification of the First 11 Years of IRI's Seasonal Climate Forecasts, J Appl Meteorol Clim,
408 49, 493-520, 10.1175/2009jamc2325.1, 2010.
409 Choi, J., Son, S. W., Ham, Y. G., Lee, J. Y., and Kim, H. M.: Seasonal-to-Interannual
410 Prediction Skills of Near-Surface Air Temperature in the CMIP5 Decadal Hindcast
411 Experiments, J Clim, 29, 1511-1527, 10.1175/Jcli-D-15-0182.1, 2016.
412 Choudhury, D., Sharma, A., Sivakumar, B., Sen Gupta, A., and Mehrotra, R.: On the
413 predictability of SSTA indices from CMIP5 decadal experiments, Environ Res Lett, 10,
414 074013, 10.1088/1748-9326/10/7/074013, 2015.
415 Dee, D. P., Uppala, S. M., Simmons, A. J., Berrisford, P., Poli, P., Kobayashi, S., Andrae, U.,
416 Balmaseda, M. A., Balsamo, G., Bauer, P., Bechtold, P., Beljaars, A. C. M., van de Berg, L.,
417 Bidlot, J., Bormann, N., Delsol, C., Dragani, R., Fuentes, M., Geer, A. J., Haimberger, L.,
418 Healy, S. B., Hersbach, H., Holm, E. V., Isaksen, L., Kallberg, P., Kohler, M., Matricardi, M.,
419 McNally, A. P., Monge-Sanz, B. M., Morcrette, J. J., Park, B. K., Peubey, C., de Rosnay, P.,
420 Tavolato, C., Thepaut, J. N., and Vitart, F.: The ERA-Interim reanalysis: configuration and
421 performance of the data assimilation system, Q J R Meteorolog Soc, 137, 553-597,
422 10.1002/qj.828, 2011.
423 Delworth, T. L., Broccoli, A. J., Rosati, A., Stouffer, R. J., Balaji, V., Beesley, J. A., Cooke,
424 W. F., Dixon, K. W., Dunne, J., Dunne, K. A., Durachta, J. W., Findell, K. L., Ginoux, P.,
425 Gnanadesikan, A., Gordon, C. T., Griffies, S. M., Gudgel, R., Harrison, M. J., Held, I. M.,
426 Hemler, R. S., Horowitz, L. W., Klein, S. A., Knutson, T. R., Kushner, P. J., Langenhorst, A.
427 R., Lee, H. C., Lin, S. J., Lu, J., Malyshev, S. L., Milly, P. C. D., Ramaswamy, V., Russell, J.,
428 Schwarzkopf, M. D., Shevliakova, E., Sirutis, J. J., Spelman, M. J., Stern, W. F., Winton, M.,
429 Wittenberg, A. T., Wyman, B., Zeng, F., and Zhang, R.: GFDL's CM2 global coupled climate
430 models. Part I: Formulation and simulation characteristics, J Clim, 19, 643-674,
431 10.1175/Jcli3629.1, 2006.
432 Ding, Y.: Seasonal march of the East-Asian summer monsoon., in: East Asian Monsoon,
433 edited by: Chang, C.-P., World Scientific, Singapore, 560, 2004.
434 Ding, Y. H.: Monsoons over China, Kluwer Academic Publisher, Dordrecht/Boston/London,
435 419 pp., 1994.
436 Ding, Y. H., and Chan, J. C. L.: The East Asian summer monsoon: an overview, Meteorol
437 Atmos Phys, 89, 117-142, 10.1007/s00703-005-0125-z, 2005.
438 Drosdowsky, W., and Zhang, H.: Verification of Spatial Fields, in: Forecast Verification: A
439 Practitioner's Guide in Atmospheric Science edited by: Jolliffe, L. T., and Stephenson, D. B.,
440 John Wiley & Sons Ltd, England, 128-129, 2003.
441 Goddard, L., Mason, S. J., Zebiak, S. E., Ropelewski, C. F., Basher, R., and Cane, M. A.:
442 Current approaches to seasonal-to-interannual climate predictions, Int J Climatol, 21, 1111-
443 1152, 10.1002/joc.636, 2001.
444 Huang, B. Y., Banzon, V. F., Freeman, E., Lawrimore, J., Liu, W., Peterson, T. C., Smith, T.
445 M., Thorne, P. W., Woodruff, S. D., and Zhang, H. M.: Extended Reconstructed Sea Surface

14

446   Temperature Version 4 (ERSST.v4). Part I: Upgrades and Intercomparisons, J Clim, 28, 911-
447   930, 10.1175/Jcli-D-14-00006.1, 2015.
448   Jiang, X. W., Yang, S., Li, Y. Q., Kumar, A., Liu, X. W., Zuo, Z. Y., and Jha, B.: Seasonal-
449   to-Interannual Prediction of the Asian Summer Monsoon in the NCEP Climate Forecast
450   System Version 2, J Clim, 26, 3708-3727, 10.1175/Jcli-D-12-00437.1, 2013.
451   Jin, E. K., Kinter, J. L., Wang, B., Park, C. K., Kang, I. S., Kirtman, B. P., Kug, J. S., Kumar,
452   A., Luo, J. J., Schemm, J., Shukla, J., and Yamagata, T.: Current status of ENSO prediction
453   skill in coupled ocean–atmosphere models, Clim Dyn, 31, 647-664, 10.1007/s00382-008-
454   0397-3, 2008.
455   Kang, I.-S., and Shukla, J.: Dynamic seasonal prediction and predictability of the monsoon,
456   in: The Asian Monsoon, edited by: Wang, B., Springer Berlin Heidelberg, Berlin, Heidelberg,
457   585-612, 2006.
458   Kang, I. S., and Yoo, J. H.: Examination of multi-model ensemble seasonal prediction
459   methods using a simple climate system, Clim Dyn, 26, 285-294, 10.1007/s00382-005-0074-8,
460   2006.
461   Kim, H. J., Wang, B., and Ding, Q. H.: The Global Monsoon Variability Simulated by
462   CMIP3 Coupled Climate Models, J Clim, 21, 5271-5294, 10.1175/2008jcli2041.1, 2008.
463   Kim, H. J., Takata, K., Wang, B., Watanabe, M., Kimoto, M., Yokohata, T., and Yasunari, T.:
464   Global Monsoon, El Nino, and Their Interannual Linkage Simulated by MIROC5 and the
465   CMIP3 CGCMs, J Clim, 24, 5604-5618, 10.1175/2011jcli4132.1, 2011.
466   Kim, H. M., Webster, P. J., Curry, J. A., and Toma, V. E.: Asian summer monsoon prediction
467   in ECMWF System 4 and NCEP CFSv2 retrospective seasonal forecasts, Clim Dyn, 39,
468   2975-2991, 10.1007/s00382-012-1470-5, 2012.
469   Kug, J. S., Kang, I. S., and Choi, D. H.: Seasonal climate predictability with Tier-one and
470   Tier-two prediction systems, Clim Dyn, 31, 403-416, DOI 10.1007/s00382-007-0264-7, 2008.
471   Lee, J.-Y., Wang, B., Kang, I. S., Shukla, J., Kumar, A., Kug, J. S., Schemm, J. K. E., Luo, J.
472   J., Yamagata, T., Fu, X., Alves, O., Stern, B., Rosati, T., and Park, C. K.: How are seasonal
473   prediction skills related to models' performance on mean state and annual cycle?, Clim Dyn,
474   35, 267-283, 10.1007/s00382-010-0857-4, 2010.
475   Luo, J.-J., Masson, S., Behera, S. K., and Yamagata, T.: Extended ENSO Predictions Using a
476   Fully Coupled Ocean–Atmosphere Model, J Clim, 21, 84-93, 10.1175/2007jcli1412.1, 2008.
477   Magnusson, L., Alonso-Balmaseda, M., Corti, S., Molteni, F., and Stockdale, T.: Evaluation
478   of forecast strategies for seasonal and decadal forecasts in presence of systematic model
479   errors, Clim Dyn, 41, 2393-2409, 10.1007/s00382-012-1599-2, 2013.
480   Matei, D., Pohlmann, H., Jungclaus, J., Muller, W., Haak, H., and Marotzke, J.: Two Tales of
481   Initializing Decadal Climate Prediction Experiments with the ECHAM5/MPI-OM Model, J
482   Clim, 25, 8502-8523, 10.1175/Jcli-D-11-00633.1, 2012.
483   Meehl, G., Covey, C., Delworth, T., Latif, M., McAvaney, B., Mitchell, J., Stouffer, R., and
484   Taylor, K.: The WCRP CMIP3 multi-model dataset: a new era in climate change research,
485   Bull Am Meteorol Soc, 88, 1383-1394, 2007.
486   Meehl, G. A., Goddard, L., Murphy, J., Stouffer, R. J., Boer, G., Danabasoglu, G., Dixon, K.,
487   Giorgetta, M. A., Greene, A. M., Hawkins, E., Hegerl, G., Karoly, D., Keenlyside, N.,
488   Kimoto, M., Kirtman, B., Navarra, A., Pulwarty, R., Smith, D., Stammer, D., and Stockdale,
489   T.: DECADAL PREDICTION Can It Be Skillful?, Bull Am Meteorol Soc, 90, 1467-1485,
490   10.1175/2009bams2778.1, 2009.
491   Meehl, G. A., and Teng, H. Y.: Case studies for initialized decadal hindcasts and predictions
492   for the Pacific region, Geophys Res Lett, 39, L22705, 10.1029/2012gl053423, 2012.
493   Meehl, G. A., Goddard, L., Boer, G., Burgman, R., Branstator, G., Cassou, C., Corti, S.,
494   Danabasoglu, G., Doblas-Reyes, F., Hawkins, E., Karspeck, A., Kimoto, M., Kumar, A.,
15

495   Matei, D., Mignot, J., Msadek, R., Navarra, A., Pohlmann, H., Rienecker, M., Rosati, T.,
496   Schneider, E., Smith, D., Sutton, R., Teng, H. Y., van Oldenborgh, G. J., Vecchi, G., and
497   Yeager, S.: DECADAL CLIMATE PREDICTION An Update from the Trenches, Bull Am
498   Meteorol Soc, 95, 243-267, 10.1175/Bams-D-12-00241.1, 2014.
499   Mitchell, J. F. B., Karoly, D. J., Hegerl, G. C., Zwiers, F. W., Allen, M. R., and Marengo, J.:
500   Detection of Climate Change and Attribution of Causes, in: Third Assessment Report of the
501   Intergovernmental Panel on Climate Change., edited by: Houghton, J. T., Griggs, D. J.,
502   Noguer, M., van der Linden, P. J., Dai, X., Maskell, K., and Johnson, C. A., Cambridge
503   University Press, New York, 470, 2001.
504   Seo, K. H., Son, J. H., Lee, J. Y., and Park, H. S.: Northern East Asian Monsoon Precipitation
505   Revealed by Airmass Variability and Its Prediction, J Clim, 28, 6221-6233, 10.1175/Jcli-D-
506   14-00526.1, 2015.
507   Smith, D. M., Eade, R., and Pohlmann, H.: A comparison of full-field and anomaly
508   initialization for seasonal to decadal climate prediction, Clim Dyn, 41, 3325-3338,
509   10.1007/s00382-013-1683-2, 2013.
510   Sperber, K., Annamalai, H., Kang, I. S., Kitoh, A., Moise, A., Turner, A., Wang, B., and
511   Zhou, T.: The Asian summer monsoon: an intercomparison of CMIP5 vs. CMIP3 simulations
512   of the late 20th century, Clim Dyn, 41, 2711-2744, 10.1007/s00382-012-1607-6, 2013.
513   Sperber, K. R., Brankovic, C., Deque, M., Frederiksen, C. S., Graham, R., Kitoh, A.,
514   Kobayashi, C., Palmer, T., Puri, K., Tennant, W., and Volodin, E.: Dynamical seasonal
515   predictability of the Asian summer monsoon, Mon Weather Rev, 129, 2226-2248,
516   10.1175/1520-0493(2001)129<2226:Dspota>2.0.Co;2, 2001.
517   Tao, S. Y., and Chen, L. X.: A review of recent research on the East Asian summer monsoon
518   in China, in: Monsoon Meterology, edited by: Chang, C.-P., and Krishnamurti, T. N., Oxford
519   University Press, Oxford, 60-92, 1987.
520   Tatebe, H., Ishii, M., Mochizuki, T., Chikamoto, Y., Sakamoto, T. T., Komuro, Y., Mori, M.,
521   Yasunaka, S., Watanabe, M., Ogochi, K., Suzuki, T., Nishimura, T., and Kimoto, M.: The
522   Initialization of the MIROC Climate Models with Hydrographic Data Assimilation for
523   Decadal Prediction, J Meteorol Soc Japan, 90a, 275-294, 10.2151/jmsj.2012-A14, 2012.
524   Taylor, K. E., Stouffer, R. J., and Meehl, G. A.: An Overview of CMIP5 and the Experiment
525   Design, Bull Am Meteorol Soc, 93, 485-498, 10.1175/Bams-D-11-00094.1, 2012.
526   Wang, B., and Xie, X.: Low-Frequency Equatorial Waves in Vertically Sheared Zonal Flow.
527   Part I: Stable Waves, J Atmos Sci, 53, 449-467, 10.1175/1520-
528   0469(1996)053<0449:lfewiv>2.0.co;2, 1996.
529   Wang, B., and Fan, Z.: Choice of south Asian summer monsoon indices, Bull Am Meteorol
530   Soc, 80, 629-638, 10.1175/1520-0477(1999)080<0629:Cosasm>2.0.Co;2, 1999.
531   Wang, B., Wu, R. G., and Fu, X. H.: Pacific-East Asian teleconnection: how does ENSO
532   affect East Asian climate?, J Clim, 13, 1517-1536, 2000.
533   Wang, B., Wu, R., and Li, T.: Atmosphere–Warm Ocean Interaction and Its Impacts on
534   Asian–Australian Monsoon Variation*, J Clim, 16, 1195-1211, 10.1175/1520-
535   0442(2003)16<1195:aoiaii>2.0.co;2, 2003.
536   Wang, B., Kang, I.-S., and Lee, J.-Y.: Ensemble Simulations of Asian–Australian Monsoon
537   Variability by 11 AGCMs*, J Clim, 17, 803-818, 10.1175/1520-
538   0442(2004)017<0803:esoamv>2.0.co;2, 2004.
539   Wang, B., Ding, Q. H., Fu, X. H., Kang, I. S., Jin, K., Shukla, J., and Doblas-Reyes, F.:
540   Fundamental challenge in simulation and prediction of summer monsoon rainfall, Geophys
541   Res Lett, 32, L15711, 10.1029/2005gl022734, 2005.
542   Wang, B.: The Asian Monsoon, Springer Science & Business Media, Praxis, New York, NY,
543   USA, 2006.

16

544 Wang, B., Lee, J.-Y., Kang, I.-S., Shukla, J., Park, C. K., Kumar, A., Schemm, J., Cocke, S.,
545 Kug, J. S., Luo, J. J., Zhou, T., Wang, B., Fu, X., Yun, W. T., Alves, O., Jin, E. K., Kinter, J.,
546 Kirtman, B., Krishnamurti, T., Lau, N. C., Lau, W., Liu, P., Pegion, P., Rosati, T., Schubert,
547 S., Stern, W., Suarez, M., and Yamagata, T.: Advance and prospectus of seasonal prediction:
548 assessment of the APCC/CliPAS 14-model ensemble retrospective seasonal prediction
549 (1980–2004), Clim Dyn, 33, 93-117, 10.1007/s00382-008-0460-0, 2008a.
550 Wang, B., Wu, Z. W., Li, J. P., Liu, J., Chang, C. P., Ding, Y. H., and Wu, G. X.: How to
551 measure the strength of the East Asian summer monsoon, J Clim, 21, 4449-4463,
552 10.1175/2008jcli2183.1, 2008b.
553 Wang, B., Xiang, B., and Lee, J. Y.: Subtropical high predictability establishes a promising
554 way for monsoon and tropical storm predictions, Proc Natl Acad Sci U S A, 110, 2718-2722,
555 10.1073/pnas.1214626110, 2013.
556 Wang, B., Lee, J. Y., and Xiang, B. Q.: Asian summer monsoon rainfall predictability: a
557 predictable mode analysis, Clim Dyn, 44, 61-74, 10.1007/s00382-014-2218-1, 2015.
558 Wu, R. G., Hu, Z. Z., and Kirtman, B. P.: Evolution of ENSO-related rainfall anomalies in
559 East Asia, J Clim, 16, 3742-3758, 10.1175/1520-0442(2003)016<3742:Eoerai>2.0.Co;2,
560 2003.
561 Wu, T. W., Song, L. C., Li, W. P., Wang, Z. Z., Zhang, H., Xin, X. G., Zhang, Y. W., Zhang,
562 L., Li, J. L., Wu, F. H., Liu, Y. M., Zhang, F., Shi, X. L., Chu, M., Zhang, J., Fang, Y. J.,
563 Wang, F., Lu, Y. X., Liu, X. W., Wei, M., Liu, Q. X., Zhou, W. Y., Dong, M., Zhao, Q. G., Ji,
564 J. J., Li, L., and Zhou, M. Y.: An Overview of BCC Climate System Model Development and
565 Application for Climate Change Studies, J Meteorol Res-Prc, 28, 34-56, 10.1007/s13351-
566 014-3041-7, 2014.
567 Wu, Z. W., Wang, B., Li, J. P., and Jin, F. F.: An empirical seasonal prediction model of the
568 east Asian summer monsoon using ENSO and NAO, J Geophys Res Atmos, 114, D18120,
569 10.1029/2009jd011733, 2009.
570 Xiang, B., Wang, B., Yu, W., and Xu, S.: How can anomalous western North Pacific
571 Subtropical High intensify in late summer?, Geophys Res Lett, 40, 2349-2354,
572 10.1002/grl.50431, 2013.
573 Xiang, B. Q., Yu, W. D., Li, T., and Wang, B.: The critical role of the boreal summer mean
574 state in the development of the IOD, Geophys Res Lett, 38, L02710, 10.1029/2010gl045851,
575 2011.
576 Yang, S., Zhang, Z. Q., Kousky, V. E., Higgins, R. W., Yoo, S. H., Liang, J. Y., and Fan, Y.:
577 Simulations and seasonal prediction of the Asian summer monsoon in the NCEP Climate
578 Forecast System, J Clim, 21, 3755-3775, 10.1175/2008jcli1961.1, 2008.
579 Yim, S. Y., Wang, B., and Xing, W.: Prediction of early summer rainfall over South China by
580 a physical-empirical model, Clim Dyn, 43, 1883-1891, 10.1007/s00382-013-2014-3, 2014.
581 Zhou, T., Wu, B., and Wang, B.: How Well Do Atmospheric General Circulation Models
582 Capture the Leading Modes of the Interannual Variability of the Asian–Australian Monsoon?,
583 J Clim, 22, 1159-1173, 10.1175/2008jcli2245.1, 2009.
584 Zhou, T. J., and Yu, R. C.: Atmospheric water vapor transport associated with typical
585 anomalous summer rainfall patterns in China, J Geophys Res Atmos, 110, D08104,
586 10.1029/2004jd005413, 2005.

587

588   Table 1. Details of the prediction systems investigated in this study.

System	Institute	Resolution		Non-Initialisation Members	Initialisation		Reference
		Atmospheric	Oceanic	Members	Members	Type	
BCC-CSM1-1	Beijing Climate Center, China	T42L26	1lonx1.33lat L40	3	3	Full-field	Wu *et al*. (2014)
CanCM4	Canadian Centre for Climate Modelling and Analysis, Canada	T63L35	256 x 192 L40	10	10	Full-field	Arora *et al*. (2011)
GFDL-CM2p1	Geophysical Fluid Dynamics Laboratory, USA	N45L24	1lon x 0.33-1lat L50	10	10	Full-field	Delworth *et al*. (2006)
HadCM3	Met Office Hadley Centre, UK	N48L19	1.25x1.25 L20	10	10 + 10	Full-field and Anomaly	Smith *et al*. (2013)
MIROC5	Atmosphere and Ocean Research Institute, Japan	T85L40	256x192 L44	5	6	Anomaly	Tatebe *et al*. (2012)
MPI-ESM-LR	Max Planck Institute for Meteorology, Germany	T63L47	GR15 L40	3	3	Anomaly	Matei *et al*. (2012)

589

18

590 Table 2. Brief summaries of initialisation strategies used by modelling groups in the study. ECMWF: European Centre for Medium-Range
591 Weather Forecasts; GODAS: Global Ocean Data Assimilation System; NCEP: National Centers for Environmental Prediction; S: Salinity;
592 SODA: Simple Ocean Data Assimilation; T: Temperature.

| system	Atmosphere	Ocean	Initialised date	Internet
BCC-CSM1-1	-	integration with ocean T nudged to SODA product above 1500 m	Ensemble 1: 1st September Ensemble 2: 1st November Ensemble 3: 1st January	http://forecast.bcccsm.ncc-cma.net/
CanCM4	ECMWF re-analysis	off-line assimilation of SODA and GODAS subsurface ocean T and S adjusted to reserve model T-S	1st January	http://www.cccma.ec.gc.ca/
GFDL-CM2p1	GFDL re-analysis	assimilates observations of T, S from World Ocean Database	1st November	https://www.gfdl.noaa.gov/multidecadal-prediction-stream/
HadCM3	ECMWF re-analysis	off-line ocean re-analysis product	1st January	http://cerawww.dkrz.de/WDCC/CMIP5/
MIROC5	-	integration using observational gridded ocean T and S	1st January	http://amaterasu.ees.hokudai.ac.jp/
MPI-ESM-LR	NCEP re-analysis	off-line ocean hindcast forced with NCEP	1st January	http://cerawww.dkrz.de/WDCC/CMIP5/

593

19

594   Table 3. Description of the six variables which contribute to the EASM. The abbreviation of these variables is followed to the guidelines of
595   CMIP5.

variable	Standard name	Contribution to the EASM
pr	Precipitation	Precipitation distribution indicates the strength of EASM
psl	Mean sea surface pressure	Differences of mean sea surface pressure between land and ocean lead to EASM
ua850	Zonal winds over 850 hPa	A component of low-level cyclone which transports vapor from ocean to land
va850	Meridional winds over 850 hPa	As ua850, and contributes to Hadley's cell
va200	Meridional winds over 850 hPa	A component of upper-level Hadley's cell
ua200	Zonal winds over 850 hPa	As va200

596

597

598

599
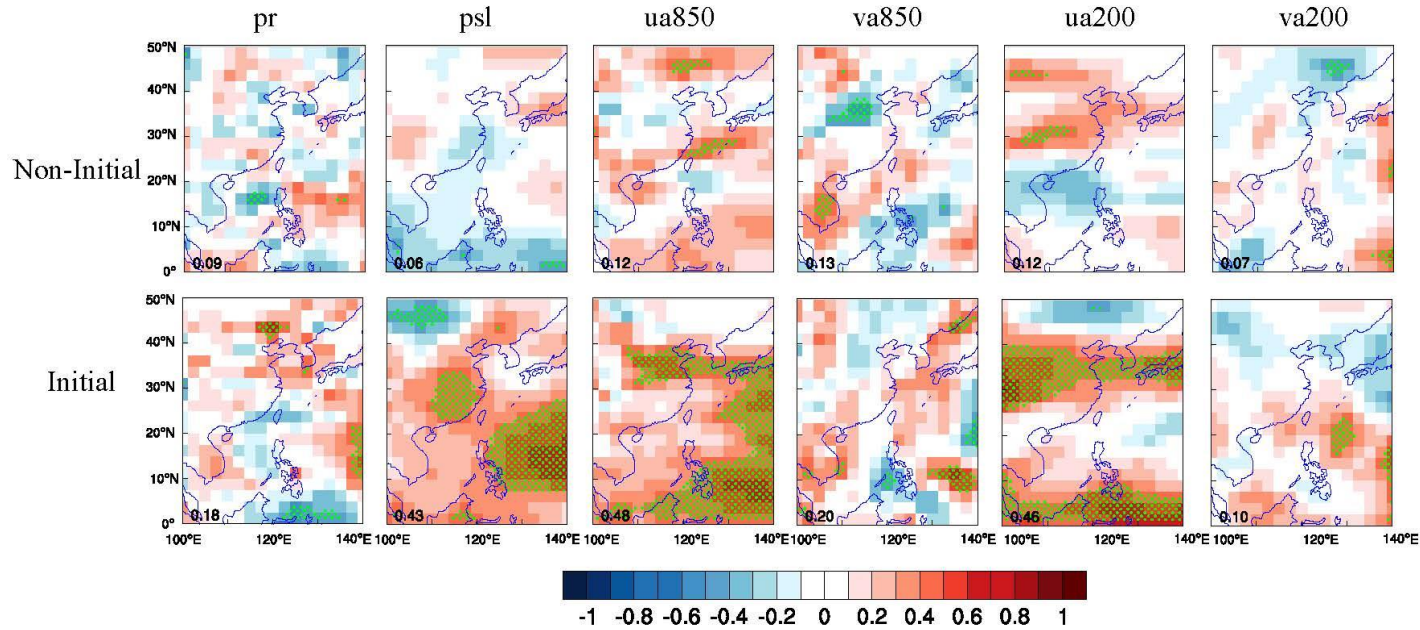
Fig. 1. Anomaly correlation coefficient of six variables (i.e. precipitation, mean sea level pressure, and winds over 850 hPa and 200 hPa) between multi-model ensemble mean and observations in non-initialisation and initialisation. The green dotted grids illustrate the significant level at 0.05. The number at lower left corner indicates the ratio of significant grid points to entire grids. The GPCP was employed as the reference data for precipitation (pr) while winds (i.e. ua850, va850, ua200 and va200) and mean sea level pressure (psl) were compared with ERA-Interim re-analysis.

21

605
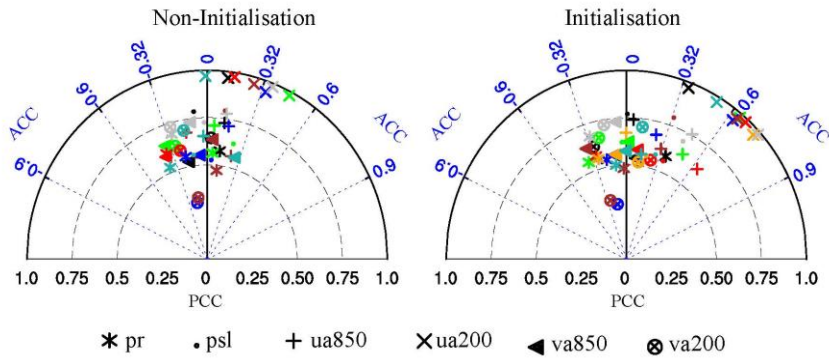
Fig.2. Taylor diagrams display of pattern (PCC) and temporal (ACC) correlation metrics of six variables between observation and model simulation in the EASM region (0-50ºN, 100-140ºE). Each coloured marker represents a model, *i.e.*, the BCC-CSM1-1 (black), the CanCM4 (green), the GFDL-CM2p1 (red), the HadCM3 (blue), the MIROC5 (brown), the MPI-ESM-LR (light-sea-blue), and the HadCM3-ff (orange).

22

614
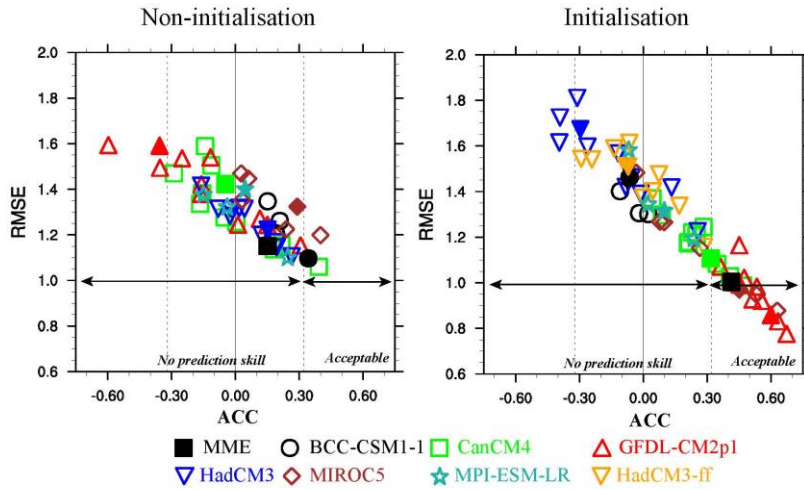
Fig. 3. Performance of the model ensemble member (hollow marker) and its ensemble
mean (solid marker) on the EASM index. The abscissa and ordinates are the anomaly
correlation coefficient (ACC) and the root-mean-square-error (RMSE), respectively.
The observed EASM index is calculated by zonal wind at 850 hPa from the ERA-
Interim re-analysis data. The black dot lines indicate the significant level at 0.1. The
vertical black line represents the correlation between the simulating and the
observational EASM index is 0.

23

623
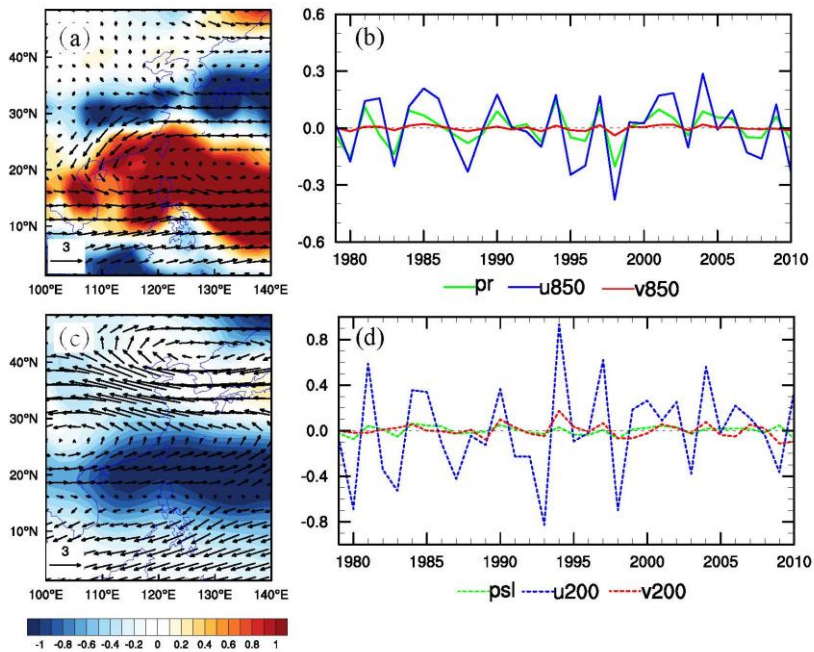
Fig. 4. Spatial distribution of observational of the first leading EOF mode of June-July-August precipitation and winds over 850 hPa (a), mean sea level pressure and winds over 200 hPa (c) and the associated principal component (PC; b, d). The GPCP and ERA-Interim data from 1979-2005 were used for the EOF analysis in the EASM domain.

629

24

630

631



632
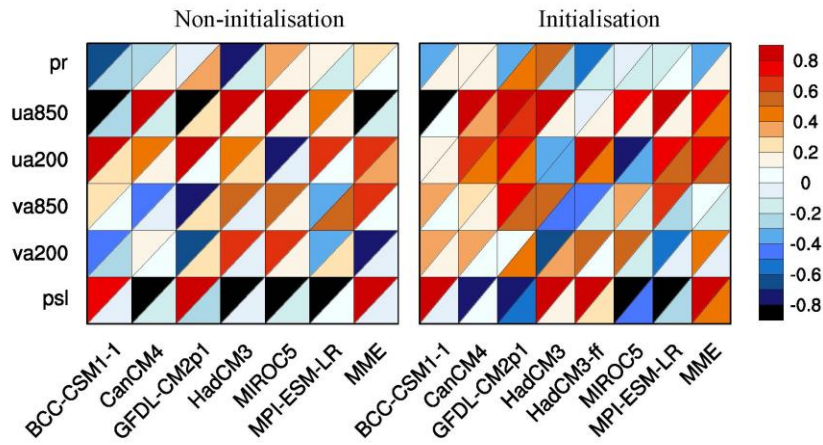
Fig. 5. Portrait diagram display of correlation metrics between the observation and the model simulation of the first lead EOF mode for the six fields in the non-initialisation (left) and the initialisation (right). Each grid square is split by a diagonal in order to show the correlation with respect to both the eigenvector (upper left triangle) and its associated principal components (lower right triangle) reference data sets.
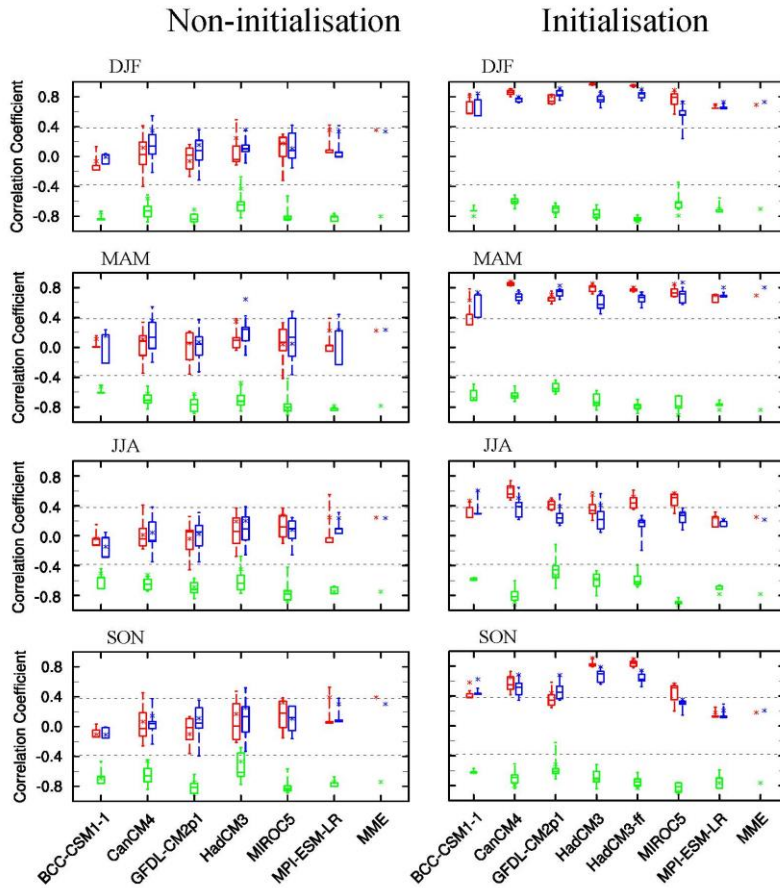
638

639
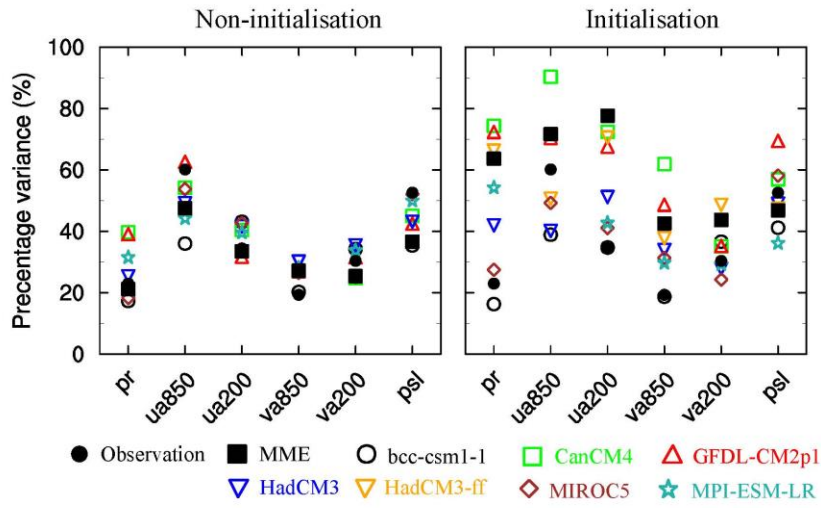
Fig. 6. Fraction variance (%) explained by the first EOF mode for six fields in the non-initialisation (left) and the initialisation (right).

640

641

642

643

Non-initialisation   Initialisation

Fig. 7. Model prediction skill in representing the observational Niño3.4 (red), the SOI (blue) from the DJF to SON in non-initialisation (left) and initialisation (right). Green diagram shows the correlation coefficient between the model simulated Niño3.4 and the SOI. Box and whisker diagram shows ensemble mean of each model (asterisk), median (horizontal line), 25th and 75th percentiles (box), minimum and maximum (whisker). The two black dotted lines indicate 0.05 significant level based upon Student's t-test.

644

645
646
647
648
649
650
651

652

653

27

654

655
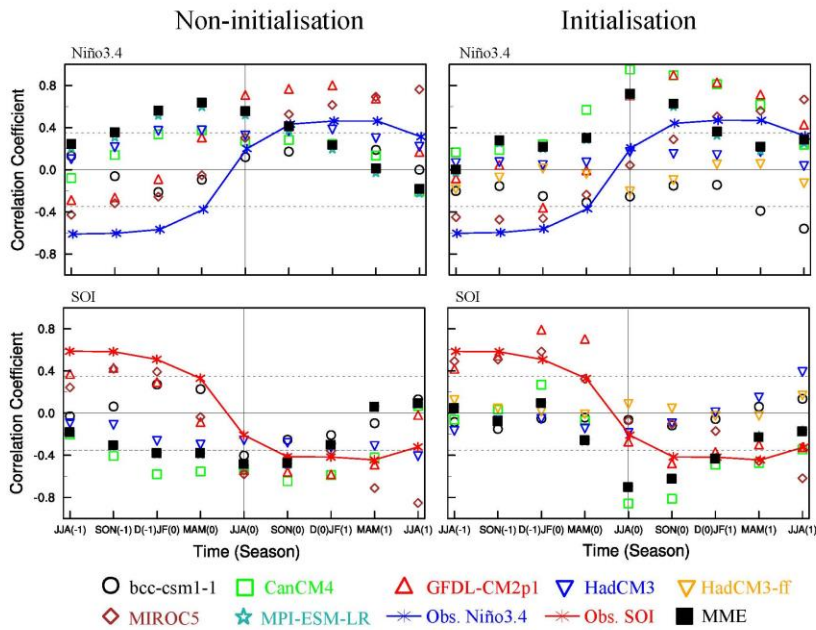
Fig. 8. Lead-lag correlation coefficients between the EASM index and Niño3.4 (upper), and SOI (lower) in non-initialised simulations (left) and initialised ones (right) for observation (marker line) and models (marker) from JJA(-1) to JJA(+1). The two black dotted lines are 0.05 significant level based upon Student's t-test. The vertical line represents JJA(0), where the simultaneous correlations between the EASM index and Niño3.4, and SOI are shown.

663